BJPS

Brazilian Journal of
Pharmaceutical Sciences

http://dx.doi.org/10.1590/s2175-97902022e19519

Article

Calendula officinalis L. flower extract-mediated green synthesis of silver nanoparticles under LED light

Angélica Panichi Santos[1]; Melissa Marques Gonçalves[1]*; Barbara Justus[1]; Daniele Priscila da Silva Fardin[1]; Ana Cristina Oltramari Toledo[1]; Jane Manfron Budel[1]; Josiane Padilha de Paula[1]

[1]Postgraduate Program in Pharmaceutical Sciences, State University of Ponta Grossa, Ponta Grossa, Paraná, Brazil

Silver nanoparticles (AgNPs) are among the most known nanomaterials being used for several purposes, including medical applications. In this study, *Calendula officinalis* L. flower extract and silver nitrate were used for green synthesis of silver nanoparticles under red, green and blue light-emitting diodes. AgNPs were characterized by Ultraviolet-Visible Spectrophotometry, Field Emission Scanning Electron Microscopy, Dynamic Light Scattering, Electrophoretic Mobility, Fourier Transform Infrared Spectroscopy and X-ray Diffraction. Isotropic and anisotropic silver nanoparticles were obtained, presenting hydrodinamic diameters ranging 90 – 180 nm, polydispersity (PdI > 0.2) and moderate stability (zeta potential values around – 20 mV).

Keywords: Nanotechnology. Metal nanoparticle. Surface plasmon resonance.

INTRODUCTION

Silver nanoparticles (AgNPs) are among the most known nanomaterials being used for several purposes (Pordeli *et al*., 2018; Kumar *et al*., 2016). In medical industry, AgNPs are widely used owing to their strong broad-spectrum antimicrobial activity (Valarmathi *et al*., 2020; Ameen *et al*., 2020; Ameen *et al*., 2019; Mythili *et al*., 2018; Barrera *et al*., 2018; Hassan, Abd El-latif, 2018). The study of antimicrobial activity of metal nanoparticles is growing because of increase in bacterial resistance to classic antibiotics, e.g., β-lactam, quinolones and aminoglycosides (Garcia-Fulgueiras *et al*., 2019; Kaur, Goyal, Kumar, 2018; Buszewski *et al*., 2016; Aragon-Martinez *et al*., 2016).

Green synthesis is considered a clean, nontoxic, simple and cost effective method to get nanoparticles. Different metal nanoparticles using silver, gold, zinc, copper and titanium can be synthesized by the reduction of metal precursor salts using plant extracts (Raj, Mali, Trivedi, 2018; Sengottaiyan *et al*., 2016; Muthusamy *et al*., 2015; Sone *et al*., 2015; Bindhu, Umadevi, 2015).

Calendula officinalis L. is a plant belonging to the *Asteraceae* family that present several medicinal properties and it is used in all over the world (Mishra *et al*., 2018) due to their anti-inflammatory, antitumor, antimicrobial and wound healing activities (Emre *et al*., 2018; López-Padilla *et al*., 2017). The main *C. officinalis* flower compounds are flavonoids, terpenoids, carotenoids, coumarines, quinones, amino acids and carbohydrates (Mishra *et al*., 2018; Nicolaus *et al*., 2017).

Asteraceae extracts-mediated green synthesis of metallic nanoparticles under different treatments are found in the literature (Francis *et al*., 2018; Vijayan *et al*., 2018), but photocatalytic reactions sensitized by light-emitting diodes (LEDs) has been used to get AgNPs with improved properties (Kumar *et al*., 2016; Lee *et al*., 2014; Stamplecoskie, Scaiano, 2010). This study describes the synthesis of AgNPs from C. officinalis flower extract and silver nitrate using red, green and blue LEDs.

***Correspondence:** M. M. Gonçalves. Universidade Federal do Paraná. Av. Prefeito Lothário Meissner, 632 - 80210-170. Jardim Botânico, Curitiba, Paraná, Brazil. Phone: +5541991750311. E-mail address: melissamg1106@gmail.com
ORCID: https://orcid.org/0000-0002-6524-2188

MATERIAL AND METHODS

Material

Silver nitrate ($AgNO_3$) CAS n° 7761-88-8 was purchased from Merck (Germany). *C. officinalis* flowers of all seasons were collected from Ponta Grossa, Paraná, Brazil (-25° 05' 42.00" S / -50° 09' 42.98" W). Representative samples were deposited in the Garden of the State University of Ponta Grossa under the number 21682. Deionized water was used in all experiments.

Preparation of the C. officinalis flower extract

5 g of *C. officinalis* dried flower were weighed and washed several times with deionized water at room temperature. Then, the flowers were crushed and immersed in 100 mL of deionized water at 60-80 °C for 30 minutes. The *C. officinalis* flower extract was obtained by removing solids in simple filtration using qualitative filter paper (80 g, FITEC®) (Thema *et al.*, 2016).

Preparation of AgNPs

For green synthesis of AgNPs, a solution of *C. officinalis* flower extract in $AgNO_3$ (1 $mmol.L^{-1}$) was prepared in 1:20 ratio. This solution was exposed to red (630 nm), green (512 nm) and blue (455 nm) Light-Emitting Diodes (LEDs) light for 48 h.

The obtained AgNPs were named as follows: AgNPsR (obtained AgNPs under exposure to red LED), AgNPsG (obtained AgNPs under exposure to green LED) and AgNPsB (obtained AgNPs under exposure to blue LED).

Characterization of AgNPs

Ultraviolet-Visible Spectrophotometry

Formation, size and shape of the AgNPs were monitored by Ultraviolet-Visible (UV-Vis) Spectrophotometry (50 UV-Vis Spectrophotometer, VARIAN CARY®) in the range of 300-600 nm (Raj, Mali, Triverdi, 2018). Prior to the analysis, the samples were diluted 1:7, in deionized water.

Field Emission Scanning Electron Microscopy

Morphological analysis of AgNPs was performed on Field Emission Scanning Electron Microscopy (FE-SEM) (Mira3, TESCAN®) at 15 kV. Prior to the analysis, the AgNPs were placed on copper tapes in stubs, dried at room temperature and submitted to metallization with gold (SC7620, QUORUM®).

Hydrodynamic Diameter, Polydispersity Index and Zeta Potential analysis

Hydrodynamic Diameter and Polydispersity Index of the AgNPs were determined by Dynamic Light Scattering (DLS) and Zeta Potential was determined by electrophoretic mobility (Zetasizer Nano ZS90, MALVERN®) in three times (T = 0 day, T = 30 days and T = 60 days) to stability evaluation. Prior to the analysis, the samples were diluted 1:20, in deionized water.

Fourier Transform Infrared Spectroscopy

In order to confirm the presence of the *C. officinalis* flower extract in the coating of the AgNPs was used Fourier Transform Infrared (FTIR) Spectroscopy (IRPrestige-21, SHIMADZU®) in the range of 4000-400 cm^{-1} in 64 scans with 4 cm^{-1} resolution and potassium bromide pallet method (Kumar *et al.*, 2016). Prior to the analysis, the AgNPs were centrifuged three times for 30 minutes at 18,000 rpm and then freeze-dried.

X-ray Diffraction

X-ray Diffraction (XRD) analysis of the AgNPs were realized in a X-ray diffractometer (XRD-6000, SHIMADZU®) employing 40 Kv, 30 mA, Cu kα radiation (λ = 1,5418 Å), 2θ from 10° to 100° and scan of $1°.min^{-1}$. Prior to the analysis, the AgNPs were centrifuged five times for 20 minutes at 18,000 rpm and then freeze-dried.

RESULTS AND DISCUSSION

During preparation of the formulations there was a change of color from pale yellow to reddish brown, indicating that *C. officinalis* flower extract compounds were able to promote the reduction of silver from Ag^{+1} to Ag^{0}, forming AgNPs (Baghizadeh *et al.*, 2015).

Formation, size and shape of AgNPs can be characterized by UV-Vis spectroscopy (Baghizadeh *et al.*, 2015) since AgNPs show optical absorption, named surface plasmon resonances, at wavelengths of 350-500 nm (Bindhu, Umadevi, 2015; Pal, Tak, Song, 2007). The larger is the nanoparticles, the greater is the wavelength of maximum absorbance and the bands intensity. The wavelength of maximum absorbance also varies according to the different AgNPs shapes (Khan *et al.*, 2011; Bhui *et al.*, 2009; Pal, Tak, Song, 2007).

According to Mie's theory, a single plasmon absorption band is expected in the spectra of spherical nanoparticles, whereas more than one plasmon absorption bands are expected in the spectra of anisotropic nanoparticles (Pal, Tak, Song, 2007). Figure 1 shows the plasmon absorption bands of AgNPs obtained using LEDs.

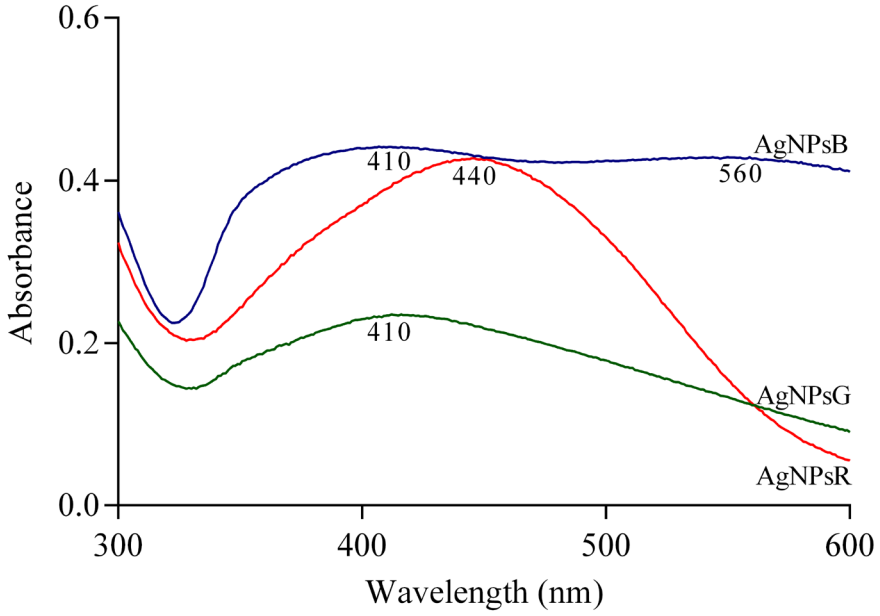

FIGURE 1 - UV-Vis spectra of AgNPs plasmon absorption bands.

The AgNPsR presented plasmon absorption band at 440 nm and the FE-SEM image showed the obtaining of spherical nanoparticles (Figure 2A). Chidambaram *et al.* (2014) and Baghizadeh *et al.* (2015) also used *C. officinalis* flower extract in green synthesis and obtained AgNPs with plasmon absorption band around 440 nm. The AgNPsG presented plasmon absorption bands at 410 nm and the FE-SEM images showed the obtaining of anisotropic nanoparticles (Figure 2B). The AgNPsB presented plasmon absorption bands at 410 and 560 nm and the FE-SEM images showed the obtaining of spherical and anisotropic nanoparticles (Figure 2C).

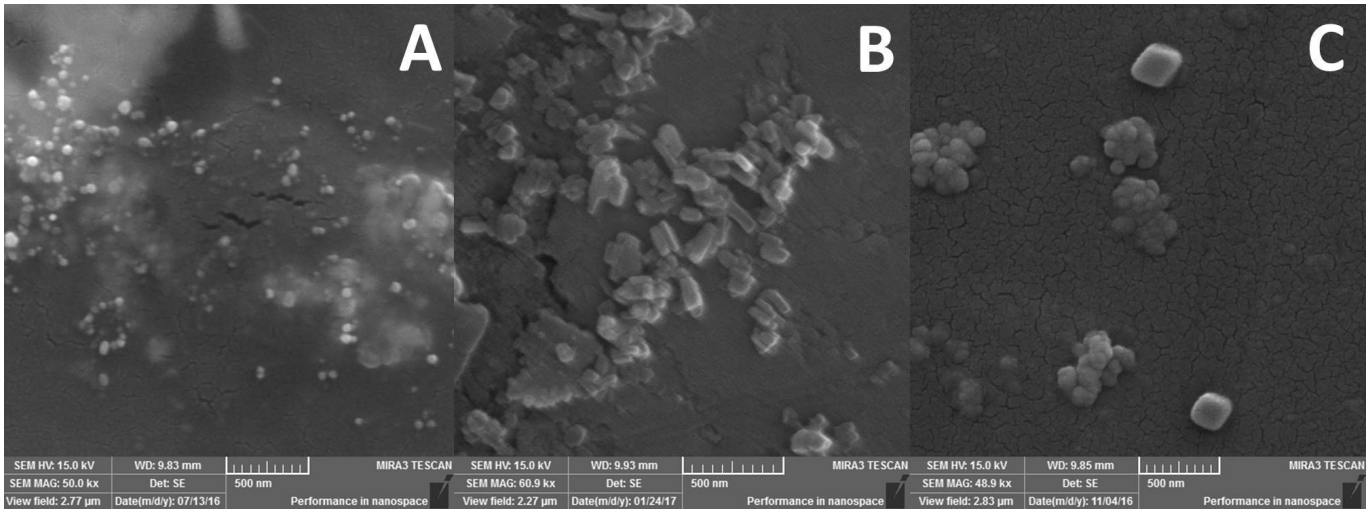

FIGURE 2 - FE-SEM images of A) AgNPsR; B) AgNPsG and C) AgNPsB.

Table I shows that the use of red LED resulted in smaller nanoparticles than the use of green and blue LEDs. However, the hydrodynamic diameters values obtained for all AgNPs produced were higher than the hydrodynamic diameters values found in the literature for AgNPs obtained by green synthesis without LEDs (Baghizadeh *et al*., 2015; Bindhu, Umadevi, 2015; Bhui *et al*., 2009).

All dispersions showed polydispersity (PdI > 0.2) (Soema *et al*., 2015) and moderate stability once presented zeta potential values around - 20 mV (Coviello *et al*., 2015). The negative zeta potential values obtained can be attributed to the *C. officinalis* flower extract compounds.

After 60 days, AgNPsR increased by 111,71% their hydrodynamic diameters, AgNPsG increased by 52,77% and AgNPsB increased by 35,49%. However, the zeta potential values remained very close to the initial values, evidencing the maintenance of stability.

The AgNPs FTIR spectra showed the same bands found in the *C. officinalis* flower extract spectrum (Figure 3 and Table II), confirming the presence of the *C. officinalis* flower extract in the coating of the AgNPs. However, a new C=O band of cetone groups appeared at 1722-1716 cm^{-1} in the AgNPs spectra, which may be result of a reduction reaction. Bands on ~1060 cm^{-1} suggest terpenoid or flavonoid compounds (Rad, Mokhtari, Abbasi, 2018; Hosseinkazemi *et al*., 2015).

In the Figure 4, *C. officinalis* flower extract diffractogram showed no crystalline planes. In contrast, the AgNPs diffractograms exhibit a typical X-ray diffraction pattern of crystal structures of silver, with peaks in 37˚-38˚, 44˚-46˚, 64˚-65˚ and 76 ˚-77˚, which correspond to crystallographic planes (111), (200), (220) and (311), respectively (Yang, Dennis, Sardar, 2011). These results are similar to those found in the literature (Baghizadeh *et al*., 2015; Bindhu, Umadevi, 2015).

(continues on the next page...)

TABLE I - Hydrodynamic Diameter (HD), Polydispersity Index (PdI) and Zeta Potential (PZ) of AgNPs at three times

AgNPs	DAY 0			DAY 30			DAY 60		
	HD (nm) ± SD	PdI ± SD	PZ (mV) ± SD	HD (nm) ± SD	PdI ± SD	PZ (mV) ± SD	HD (nm) ± SD	PdI ± SD	PZ (mV) ± SD
AgNPsR	88,62 ± 6,02	0,530 ± 0,028	-22,86 ± 1,48	103,35 ± 18,63	0,445 ± 0,257	-20,96 ± 0,77	187,62 ± 2,60	0,611 ± 0,014	-18,5 ± 0,707
AgNPsG	138,11 ± 5,52	0,468 ± 0,037	-21,00 ± 1,44	201,10 ± 21,52	0,487 ± 0,102	-21,40 ± 1,44	211,00 ± 26,00	0,453 ± 0,050	-19,2 ± 2,80
AgNPsB	175,43 ± 21,25	0,510 ± 0,035	-17,33 ± 2,08	246,01 ± 26,25	0,463 ± 0,046	-16,01 ± 4,08	237,70 ± 23,30	0,570 ± 0,205	-17,10 ± 0,84

SD: Standard Deviation.

TABLE II - Wavenumber (cm^{-1}) and its corresponding chemical structure of FTIR spectra of AgNPsR, AgNPsG, AgNPsB and *C. officinalis* flower extract

***C. officinalis* flower extract**		**AgNPsR**		**AgNPsG**		**AgNPsB**	
Wavenumber (cm^{-1})	**Chemical Structure**	**Wavenumber (cm^{-1})**	**Chemical Structure**	**Wavenumber (cm^{-1})**	**Chemical Structure**	**Wavenumber (cm^{-1})**	**Chemical Structure**
3398	O-H	3398	O-H	3398	O-H	3398	O-H
2936	C-H	2993	C-H	2993	C-H	2936	C-H
1622	C=O	1722	C=O	1716	C=O	1717	C=O
1405	C=C	1625	C=O	1630	C=O	1633	C=O
1265	C-H	1389	C=C	1384	C=C	1393	C=C
1065	C-O	1063	C-O	1062	C-O	1060	C-O

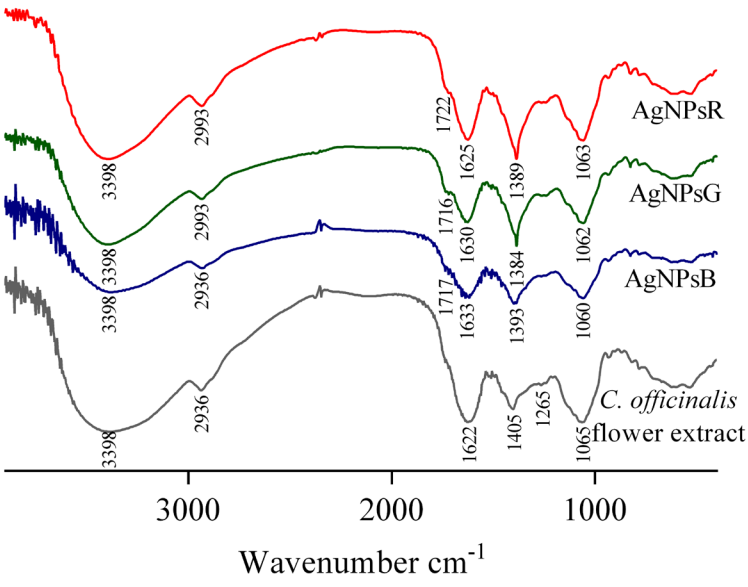

FIGURE 3 - FTIR spectra of AgNPsR, AgNPsG, AgNPsB and *C. officinalis* flower extract.

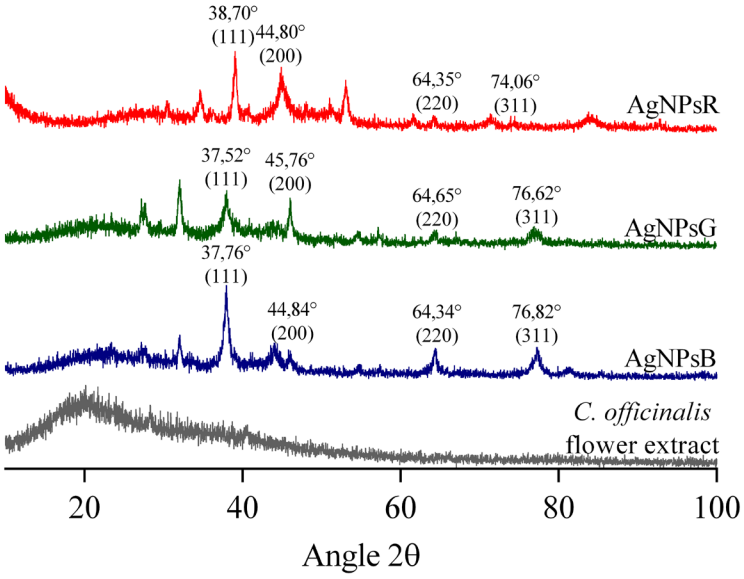

FIGURE 4 - XRD patterns of AgNPsR, AgNPsG, AgNPsB and *C. officinalis* flower extract.

CONCLUSION

Were obtained isotropic and anisotropic AgNPs with hydrodynamic diameters of 89 to 175 nm from C. officinalis flower extract and $AgNO_3$ under red, green and blue LED. AgNPs remained stable during the evaluated period with potential zeta values around -20 mV, but increased their hydrodynamic diameters considering that AgNPsB showed a smaller increase than AgNPsR and AgNPsG. AgNPs with required properties can be produced from the proposed method in order to be used as antimicrobial in health products.

ACKNOWLEGEMENTS

The authors would like to thank C-LABMU/PROPESP - UEPG for characterization of silver nanoparticles analysis. This study was financed in part by the Coordenação de Aperfeiçoamento de Pessoal de Nível Superior - Brasil (CAPES) - Finance Code 001.

REFERENCES

Ameen F, AlYahia S, Govarthanan M, ALjahdali N, Al-Enazi N, Alsamhari K, et al. Soil bacteria *Cupriavidus sp.* mediates the extracellular synthesis of antibacterial silver nanoparticles. J Mol Struct. 2020;1202:127233.

Ameen F, Srinivasan P, Selvankumar T, Kamala-Kannan S, Al Nadhari S, Almansob A, et al. Phytosynthesis of silver nanoparticles using *Mangifera indica* flower extract as bioreductant and its broad-spectrum antibacterial activity. Bioorg Chem. 2019;88:102970.

Aragon-Martinez OH, Isiordia-Espinoza MA, Tejeda Nava FJ, Aranda Romo S. Dental Care Professionals Should Avoid the Administration of Amoxicillin in Healthy Patients During Third Molar Surgery: Is Antibiotic Resistence the Only Problem? J Oral Maxillofac Surg. 2016;74(8):1512-1513.

Barrera N, Guerrero L, Debut A, Santa-Cruz P. Printable nanocomposites of polymers and silver nanoparticles for antibacterial devices produced by DoD technology. PLoS ONE. 2018;13(7):1-19.

Baghizadeh A, Ranjbar S, Gupta VK, Asif M, Pourseyedi S, Karimi M J et al. Green synthesis of silver nanoparticles using seed extract of *Calendula officinalis* in liquid phase. J Mol Liq. 2015;207:159-163.

Bindhu MR, Umadevi M. Antibacterial and catalytic activities of green synthesized silver nanoparticles. Spectrochim Acta Part A. 2015;135:373-378.

Bhui DK, Bar H, Sarkar P, Sahoo GP, De SP, Misha A. Synthesis and UV–vis spectroscopic study of silver nanoparticles in aqueous SDS solution. J Mol Liq. 2009;145(1):33-37.

Buszewski B, Rafinska K, Pomastowski P, Walczak J, Rogowska A. Novel aspects of silver nanoparticles functionalization. Colloids Surf A. 2016;506:170-178.

Chidambaram J, Saritha K, Maheswari R, Muzammil MS. Efficacy of Green Synthesis of Silver Nanoparticles using Flowers of *Calendula Officinalis*. Chem Sci Trans. 2014;3(2):773-777.

Coviello T, Trotta AM, Marianecci C, Carafa M, Di Marzio L, Rinaldi F, et al. Gel-embedded niosomes: Preparation, characterization and releasestudies of a new system for topical drug delivery. Colloids Surf B. 2015;125:291-299.

Emre A, Sertkaya M, İşler A, Bahar AY, Şanlı NA, Özkömeç A, et al. Comparison of the protective effects of *calendula officinalis* extract and hyaluronic acid anti-adhesion barrier against postoperative intestinal adhesion formation in rats. Turk J Colorectal Dis. 2018;28(2):88-94.

Francis S, Joseph S, Koshy EP, Mathew B. Microwave assisted green synthesis of silver nanoparticles using leaf extract of *Elephantopus scaber* and its environmental and biological applications. Artif Cells Nanomed Biotechnol. 2018;46(4):795-804.

Garcia-Fulgueiras V, Zapata Y, Papa-Ezdra R, Ávila P, Caiata L, Seija V, et al. First characterization of K. pneumoniae ST11 clinical isolates harboring bla_{KPC-3} in Latin America. Rev Argent Microbiol. 2019;367:1-6.

Hassan SWM, Abd El-latif HH. Characterization and applications of the biosynthesized silver nanoparticles by Marine *Pseudomonas* sp. H64. J Pure Appl Microbiol. 2018;12(3):1289-1299.

Hosseinkazemi H, Biazar E, Bonakdar S, Ebadi M-T, Shokrgozar M-A, Rabiee M. Modification of PCL electrospun nanofibrous mat with *Calendula officinalis* extract for improved interaction with cells. Int J Polym Mater Polym Biomater. 2015;64(9):459-464.

Kaur A, Goyal D, Kumar R. Surfactant mediated interaction of vancomycin with silver nanoparticles. Appl Surf Sci. 2018;449:23-30.

Khan Z, Al-Thabaiti SA, Obaid AY, Al-Youbi AO. Preparation and characterization of silver nanoparticles by chemical reduction method. Colloids Surf B. 2011;82(2):513-517.

Kumar B, Angulo Y, Smita K, Cumbal L, Debut A. Capuli cherry-mediated green synthesis of silver nanoparticles under white solar and blue LED light. Particuology. 2016;24:123-128.

Lee SW, Chang SH, Lai YS, Lin CC, Tsai CM, Lee YC, et al. Effect of temperature on the growth of silver nanoparticles using plasmon-mediated method under the irradiation of green LEDs. Materials. 2014;7(12)**:**7781-7798.

López-Padilla A, Ruiz-Rodriguez A, Reglero, G, Fornari T. Supercritical carbon dioxide extraction of *Calendula officinalis*: Kinetic modeling and scaling up study. J Supercrit Fluid. 2017;130:292-300.

Mishra AK, Mishra A, Pragya, Chattopadhyay P. Screening of acute and sub-chronic dermal toxicity of *Calendula officinalis* L essential oil. Regul Toxicol Pharmacol. 2018;98:184-189.

Muthusamy G, Praburaman L, Thangasamy S, Jong-Hoon K, Seralathan K-K, Adithan A, et al. Sunroot mediated synthesis and characterization of silver nanoparticles and evaluation of its antibacterial and rat splenocyte cytotoxic effects. Int J Nanomed. 2015;10:1977-1983.

Mythili R, Selvankumar T, Kamala-Kannan S, Sudhakar C, Ameen F, Al-Sabri A, et al. Utilization of market vegetable waste for silver nanoparticle synthesis and its antibacterial activity. Mater Lett. 2018;225:101-104.

Nicolaus C, Junghanns S, Hartmann A, Murillo R, Ganzera M, Merfort I. *In vitro* studies to evaluate the wound healing properties of *Calendula officinalis* extracts. J Ethnopharmacol. 2017;196:94-103.

Pal S, Tak YK, Song JM. Does the Antibacterial Activity of Silver Nanoparticles Depend on the Shape of the Nanoparticle? A Study of the Gram-Negative Bacterium *Escherichia coli*. Appl Environ Microbiol. 2007;73(6):1712-1720.

Pordeli HR, Shaki H, Azari AA, Nezhad MS. Biosynthesis of Silver Nanoparticles by Fusarium solani isolates from Agricultural Soils in Gorgan, Iran. Med Lab J. 2018;12(4):17-22.

Rad ZP, Mokhtari J, Abbasi M. Preparation and characterization of *Calendula officinalis*-loaded PCL/gum arabic nanocomposite scaffolds for wound healing applications. Iran Polym J. 2019;28(1):51-63.

Raj S, Mali SC, Trivedi R. Green synthesis and characterization of silver nanoparticles using *Enicostemma axillare* (Lam.) leaf extract. Biochem Biophys Res Commun. 2018;503(4):2814-2819.

Sengottaiyan A, Mythili R, Selvankumar T, Aravinthan A, Kamala-Kannan S, Manoharan K, et al. Green synthesis of silver nanoparticles using *Solanum indicum* L. and their antibacterial, splenocyte cytotoxic potentials. Res Chem Intermed. 2016;42:3095-3103.

Soema PC, Willems G-J, Jiskoot W, Amorij J-P, Kersten GF. Predicting the influence of liposomal lipid composition on liposome size, zeta potential and liposome-induced dendritic cell maturation using a design of experiments approach. Eur J Pharm Biopharm. 2015;94:427-435.

Sone BT, Manikandan E, Gurib-Fakim A, Maaza M. Sm_2O_3 nanoparticles green synthesis via *Callistemon viminalis*' extract. J Alloy Compd. 2015;650:357-362.

Stamplecoskie KG, Scaiano JC. Light Emitting Diode Irradiation Can Control the Morphology and Optical Properties of Silver Nanoparticles. J Am Chem Soc. 2010;132(6):1825-1828.

Thema FT, Manikandan E, Gurib-Fakim A, Maaza M. Single phase Bunsenite NiO nanoparticles green synthesis by *Agathosma betulina* natural extract. J Alloys Compd. 2016;657:655-661.

Valarmathi N, Ameen F, Almansob A, Kumar P, Arunprakash S, Govarthanan M. Utilization of marine seaweed *Spyridia filamentosa* for silver nanoparticles synthesis and its clinical applications. Mater Lett. 2020;263:127244.

Vijayan R, Joseph S, Mathew B. Eco-friendly synthesis of silver and gold nanoparticles with enhanced antimicrobial, antioxidant, and catalytic activities. IET Nanobiotechnol. 2018;12(6):850-856.

Yang J, Dennis RC, Sardar DK. Room-temperature synthesis of flowerlike ag nanostructures consisting of single crystalline ag nanoplates. Mater Res Bull. 2011;46(7):1080-1084.

Received for publication on 23rd July 2019
Accepted for publication on 06th May 2020